

Simulation of Fracture of Flexible Polymer Chains in Transient Elongational Flow

K. D. Knudsen, J. G. Hernández Cifre, J. J. López Cascales, and J. García de la Torre*

Departamento de Química Física, Facultad de Química, Universidad de Murcia, 30071 Murcia, Spain

Received October 12, 1994; Revised Manuscript Received March 17, 1995[®]

ABSTRACT: Using the Brownian dynamics technique, we have simulated the fracture process of flexible polymer chains subjected to convergent (sink) flow, where the elongational rate is strongly position dependent. The system studied has been a very dilute solution of polystyrene with molecular weight 2×10^6 in cyclohexane at a temperature of 35 °C. The polymer was modeled as a bead–spring chain, adequately parametrized as to reproduce real polymer/solvent conditions. The fracture yield varies with the flow rate and is seen to depend to a high degree on the instrumental setup. The distribution of fragments at the end of the convergent flow region is found to be centered around half the initial molecular weight, and we find that there is no fracture below a certain critical flow rate. These results are in qualitative agreement with the experimental results of Reese and Zimm¹ on DNA and Nguyen and Kausch² on polystyrene, a finding that confirms the applicability of the Brownian dynamics simulation technique for studying polymer chain fracture.

Introduction

It has been realized during recent years that the behavior of chain molecules in flows that have a predominant elongational, nonrotational character is qualitatively different from, for instance, that of simple shear flows. When a dilute polymer solution is subjected to an elongational flow, two interesting phenomena show up. First, when the elongation rate exceeds some critical value, the polymer chain uncoils suddenly, experiencing the so-called coil–stretch transition. Then, if the elongational rate is increased further beyond another characteristic limit, the polymer chain breaks into two pieces. These phenomena have been studied theoretically by de Gennes,³ in the laboratory by, for instance, Keller and Odell,⁴ and by computer simulation by López Cascales and García de la Torre.^{5,6} But in all these cases the situation was that of an idealized steady flow, where the elongational rate is constant in time and space.

However, the elongational flows that take place in situations of practical and technological interest are often transient flows, with a position-dependent elongational rate, so that the stress on the polymer chain varies with time. That happens when the polymer solution passes through a sudden constriction, such as in pipettes or syringes, or in porous beads. Theoretical predictions by Rabin⁷ and laboratory experiments by Reese and Zimm¹ and Nguyen and Kausch² have shown that the observations made in transient flows may show features different from what is observed in steady flows.

In the present study we have applied the Brownian dynamics technique to simulate the behavior of polymer chains in transient flows. The polymer/solvent system considered is a dilute solution of linear polymer chains in unperturbed (Θ) conditions. The polymer is modeled as a bead–spring chain which is adequately parametrized so as to reproduce real polymer/solvent conditions. In the simulations we employ a flow field of the same type as in the device used in the laboratory experiments of the aforementioned authors.^{1,2} The

present work may be regarded as a preliminary study, where the main purpose has been to investigate the applicability of the Brownian dynamics technique to study *qualitative* aspects of the fracture process.

Model and Simulation Method

The simulated system is a Θ solution of monodisperse polystyrene in cyclohexane at 35 °C. The polymer molecule is modeled as a bead–spring Rouse chain in which the behavior of the springs is Hookean, with potential energy $V = Hq^2/2$. The spring constant H equals $3kT/b^2$, and q is the instantaneous spring length. The parameter b is the root-mean-squared spring length. The parametrization of the model requires two arbitrary choices. The first one is the molecular weight per bead, M_1 , which is taken to be 10^5 . Thus, the number of beads, $N = M/M_1$, required for a polymer of a few million in molecular weight as used in experiments,² is not prohibitively high for the computer simulation. A polymer with molecular weight 2×10^6 will with this assumption be modeled as a 20-bead chain. Anyhow, it can be shown that the final results will not depend on this choice provided that N is large enough. The root-mean-squared spring length is now obtained by combining the expression for the experimental molecular weight of the radius of gyration for a flexible polymer

$$\langle S^2 \rangle = C_S M \quad (1)$$

with the theoretical expression for $\langle S^2 \rangle$ for a Rouse chain⁸

$$\langle S^2 \rangle = \frac{N^2 - 1}{6N} b^2 \approx \frac{N}{6} b^2 \quad (2)$$

Equation 1 together with eq 2 then gives

$$b^2 = 6C_S M_1 \quad (3)$$

For polystyrene in cyclohexane at 35 °C, $C_S = 7.9 \times 10^{-18} \text{ cm}^2 \text{ mol/g}$, which by means of eq 3 results in a

* To whom correspondence should be addressed.

[®] Abstract published in *Advance ACS Abstracts*, May 15, 1995.

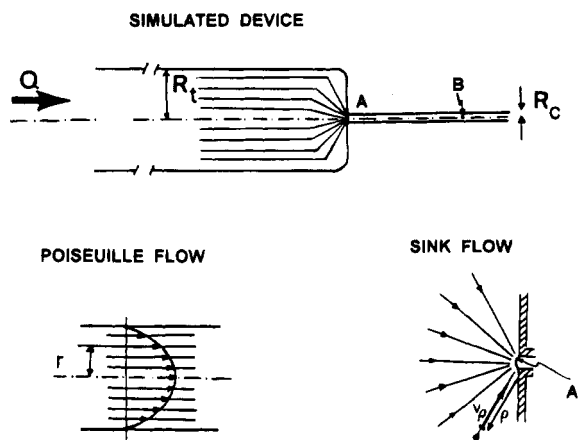


Figure 1. Cross section of the simulated device (upper figure). R_t and R_c are the radii of the cylindrical tube and the capillary, with values 1.0 and 0.02 cm, respectively. Q is the volumetric flow rate. In the cylindrical tube, we assume Poiseuille flow and, near the orifice, convergent flow (starting at a distance R_t from the orifice). At the bottom right of the figure is illustrated the radial velocity in the convergent (sink) flow region.

value of 21.7 nm for b . The hydrodynamic radius of the beads is as usual taken to be $\sigma = 0.25b$.^{5,6}

In order to simulate the fracture process, we have employed springs that break when the stretching energy reaches some limiting value, A , the spring dissociation energy, corresponding to a spring length q_{\max} . Although several alternatives are available,^{5,6} we apply here the simplest representation, with modified Hookean springs, in which the potential energy is quadratic in q until some spring length $q_{\max} = (2A/H)^{1/2}$ is reached. Beyond that, the potential energy is constant, $V = A$. The assignment of A is the second and last arbitrary choice in the model. We have found that the results may depend quantitatively on the value of A , but their trend and general conclusions are not influenced by this choice. For the present simulations we have used $A = 30$ kcal/mol.

The simulated system is shown in Figure 1. It consists of a cylindrical tube of radius $R_t = 1.0$ cm with a sudden constriction, so that the fluid passes through a very small orifice of radius $R_c = 0.02$ cm. This part of the device is inspired by the experimental setups of Reese and Zimm¹ and Nguyen and Kausch.² In our simulation, the orifice is followed by a needle or capillary, so that the whole device resembles a syringe. The volumetric flow rate through the device is denoted Q . In the cylinder we have Poiseuille (laminar) flow, and the velocity along the center line is related to the flow rate by the expression $v_c = 2Q/\pi R_t^2$. When the fluid approaches the orifice, at a distance of R_t , the streamlines converge and we have sink (convergent) flow. This flow pattern, with an abrupt change from the region of parallel to that of convergent flow, is obviously an idealization of the real flow pattern. It is, however, convenient from a modeling point of view and presumably of minor importance concerning the fracture process, since fracturing starts to take place well within the region of convergent flow. In the region of sink flow, the radial velocity (along a streamline) depends on the distance to the orifice, q , as

$$v(q) = v_0 q_0^2 / q^2 \quad (4)$$

where $q_0 = R_t$, and v_0 is the velocity in that streamline at the end of the Poiseuille region, determined by the

instrumental dimensions and the flow rate. Thus, the velocity is inversely proportional to the square of the distance to the orifice. This results from the fact that the volumetric flow rate Q is constant, whereas the cross-section area of the flow is proportional to the square of the distance from the orifice. At the entrance of the orifice (position A in the "Sink Flow" drawing in Figure 1), in our model the sink flow is considered to terminate and from this point on the flow is considered laminar. The position where the flow pattern changes is situated at a distance R_c (equal to the capillary diameter) from the origin of coordinates for the sink flow.

The elongational rate is given by the expression $|dv(q)/dq|$ and equals in the region of convergent flow

$$\epsilon(q) = 2v_0 q_0^2 / q^3 \quad (5)$$

We see that the elongational rate is strongly position dependent, which is characteristic for transient flows.

In our simulations we place the polymer chain, generated with Gaussian statistics, at a distance q_{ini} from the orifice, in the region of elongational flow. In principle, q_{ini} should be as large as it is in the macroscopic device, but this would make the Brownian dynamics simulations very time consuming. As the elongational rate at the beginning of the convergent region is rather weak, q_{ini} is placed somewhere in the middle of the region. The choice of q_{ini} will later on be discussed in terms of the residence time for the chain. This is the time that the chain is situated in the flow field before it reaches the orifice. The residence time is given by the expression

$$t_{\text{res}} = q_{\text{ini}}^3 / 3v_0 q_0^2 \quad (6)$$

We see that the residence time decreases very sharply as the chain is getting closer to the orifice.

We will later discuss results with respect to the longest relaxation time of the chain molecule. For a flexible Rouse chain, as used in our study, this is calculated from the expression⁸

$$\tau_1 = \frac{\zeta/2H}{4 \sin^2(\pi/2N)} \quad (7)$$

where $\zeta = 6\pi\eta_s\sigma$, η_s being the solvent viscosity. In our case, the number of beads (N) is equal to 20, which along with the data for the polystyrene/cyclohexane system gives a value of the primary relaxation time of the chain molecule equal to 73 μ s.

At a distance q approximately equal to the orifice radius R_c (point A), the simulation can be stopped, as in the study of Reese and Zimm.¹ Alternatively, we can simulate a syringelike device by letting the flow proceed through the constriction (needle), assuming Poiseuille flow within the needle and starting at the point where $q = R_c$ and $v = v_0 q_0^2 / R_c^2$. Inside the needle we will make use of a reference point B, separated from the orifice a distance on the order of the distance travelled by the polymer chain in a few relaxation times.

The evolution of the polymer chains as they flow through this device is simulated by employing the Brownian dynamics algorithm of Ermak and McCammon.⁹ After a Brownian step of duration Δt , the new position vector \mathbf{r}_i of a bead is obtained from the initial position \mathbf{r}_i^0 as

$$\mathbf{r}_i = \mathbf{r}_i^0 + \frac{\Delta t}{kT} \sum_j \mathbf{D}_{ij}^0 \cdot \mathbf{F}_j^0 + \mathbf{v}(\mathbf{r}_i^0) \Delta t + \mathbf{Q}_i^0 \quad (8)$$

where the superscript 0 refers to the instant when the time step begins. \mathbf{F}_j^0 is the spring force on bead j . \mathbf{D}_{ij}^0 ($i, j = 1, \dots, N$) is the ij block of the diffusion tensor. The parameter $\mathbf{v}(\mathbf{r}_i^0)$ is the velocity of the solvent at position \mathbf{r}_i^0 at the beginning of the time step. \mathbf{Q}_i is a random vector with mean value $\mathbf{0}$ and variance-covariance equal to $2\Delta t \mathbf{D}_{ij}^0$. The displacement of a bead thus has three contributions, that due to the spring forces on the bead, weighted with the diffusion coefficient, the contribution due to solvent flow, and a stochastic part due to the impulses from the random motion of the solvent molecules surrounding the bead. In the simulations the basic algorithm (eq 8) is used with a second-order modification,¹⁰ which has been shown to give improved calculation efficiency.

When hydrodynamic interaction between the chain units is taken into consideration, the Rotne-Prager-Yamakawa interaction tensor¹¹ is used for \mathbf{D}_{ij}^0 . If this interaction is neglected, \mathbf{D}_{ij}^0 is just kT/ζ , where ζ is the friction coefficient of a bead, also used in eq 7.

Trajectories are obtained by means of the above-mentioned procedure for a sample containing a sufficiently large number of chains. The time step, Δt , was in the range 10–100 ns. This value is thus much smaller than the primary relaxation time of the polymer, a necessary requirement of the simulation procedure. For the results reported here, we neglected the hydrodynamic interaction (HI) between the beads, as in other simulations in elongational flow.^{1,5,6} Neglecting the hydrodynamic interaction makes it possible to reduce substantially the computing time, thus allowing long chains and large trajectories.

In the simulations the polymer is initially placed on the center line of the device at a distance so that it will take a time larger than the relaxation time of the polymer chain to reach the orifice. Brownian trajectories were then simulated for several thousand molecules. While following the trajectory of one molecule, at each step in the simulation we monitored every spring for fracture ($q > q_{\max}$). If spring i in a chain of N springs is broken, two fragments of molecular weight $iM/(N-1)$ and $(N-i-1)M/(N-1)$ will result. Carrying out this for all the chains in the initial sample, the molecular weight distribution can be evaluated. The number of intact chains is then finally monitored at the two points A and B (Figure 1).

Results and Discussion

The results of the experimental studies of Reese and Zimm and Nguyen and Kausch present two main features. One of them is the molecular weight distribution of the fragments. In both studies the initial sample was nearly monodisperse, with molecular weight M . After passage through the orifice, the molecular weight distribution shows a peak at M , corresponding to intact chains, and a second peak centered at half of the initial value. This clearly indicates that, in those experiments,^{1,2} fracture is most likely to take place at the middle of the chain. By integration of the areas under the peaks, it was possible to determine the degradation yield, i.e., the percentage of broken chains. When plotted vs the maximum elongational rate near the orifice (or, equivalently, vs the flow rate through the device), it was observed² that no fracture took place below a certain threshold value of the flow rate and that

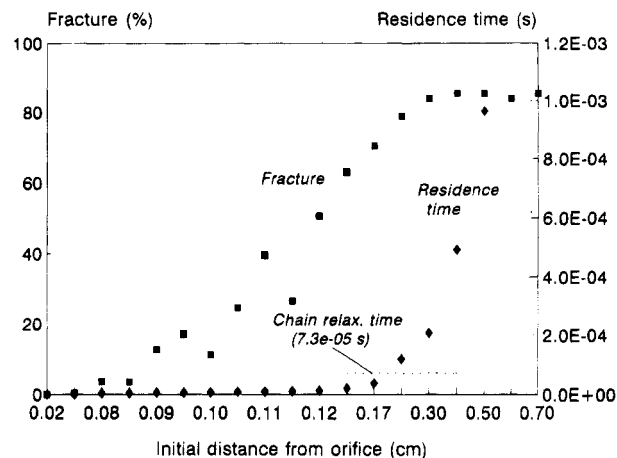


Figure 2. Percentage of chains fractured (left axis) while flowing to the orifice vs initial distance from the orifice. Volumetric flow rate (Q) = 60 cm³/s. The time that the chain is situated in the flow before it reaches the orifice is also shown (residence time, right axis). The simulated system was a very dilute solution of polystyrene ($M = 2 \times 10^6$) in cyclohexane at 35 °C.

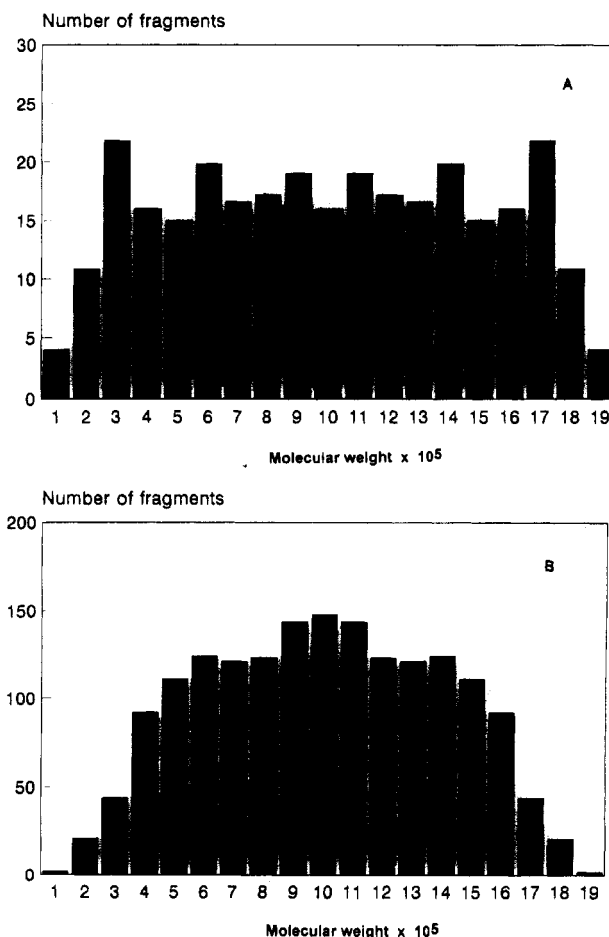


Figure 3. Distribution of molecular weight of the fracture fragments of polystyrene ($M = 2 \times 10^6$) for different initial positions of the chain. Volumetric flow rate (Q) = 60 cm³/s. (A) Initial distance from the orifice = 0.9 mm. (B) Initial distance from the orifice = 5.0 mm.

the fracture yield increased smoothly when the threshold value was exceeded.

In our simulation study we have tried to mimic the experiment of these authors. However, before looking at fracture yield vs flow rate, we wanted to study how the degradation depends on our choice of the initial

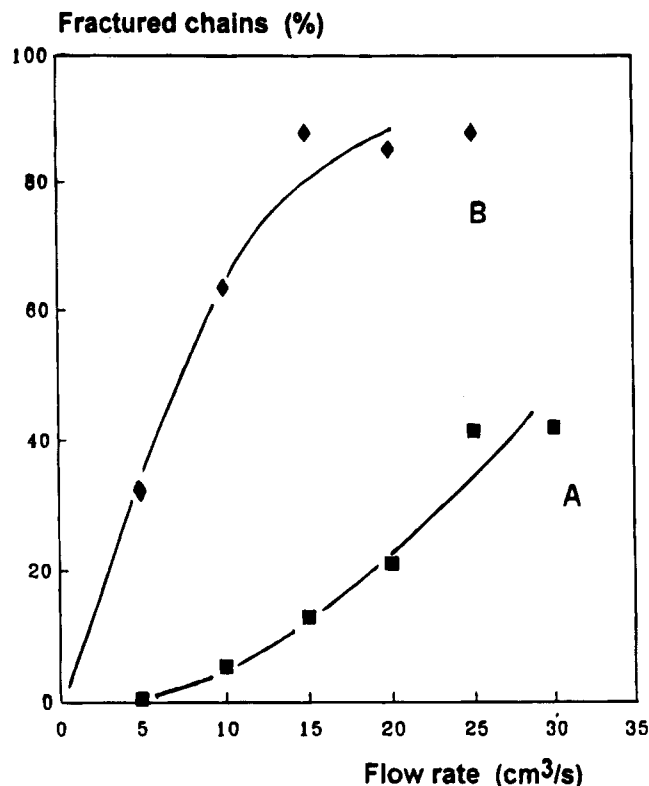


Figure 4. Fracture yield (%) of polystyrene ($M = 2 \times 10^6$) vs flow rate through the device when monitored at different positions in the simulated device. Volumetric flow rate (Q) = 25 cm³/s. (A) Fracture yield at the orifice. (B) Fracture yield inside the capillary.

position of the polymer chain in the region in front of the orifice. It seems reasonable that the fracture yield should increase as the polymer chain is allowed to experience the convergent flow during a longer period. One might also expect that the fracture yield reaches a saturation point at some value of the initial distance. We simulated Brownian trajectories for a large number of polystyrene chains with initial molecular weight 2×10^6 .

In Figure 2 is shown the fracture yield for a 20-bead chain as function of its initial distance from the orifice. We can see that, when the polymer is placed initial very close to the orifice, the fracture yield is close to zero. It then increases slowly with increasing initial distance, reaching a maximum of about 80% for the flow rate used ($Q = 60$ cm³/s). In the figure is also plotted the time that the chain is situated in the flow field before it reaches the orifice (residence time). It is seen, as mentioned earlier in connection with eq 6, how the residence time increases strongly with increasing initial distance. From this figure it is noted that the region where the residence time for the chain exceeds its primary relaxation time ($73 \mu\text{s}$) corresponds to the region where the fracture yield reaches its maximum. This is probably because fracture takes place preferentially after the unfolding of the chain, and this unfolding process is governed by, in addition to the strength of the flow field, the primary relaxation time of the molecule, being directly related to the molecular weight (eq 7). In order to stay in the saturation region (maximum fracture), the residence time should be, based on this preliminary study, at least 2 times the primary relaxation time of the chain. The different results in the literature regarding degradation yield in steady and transient flow may, to a large extent, be due

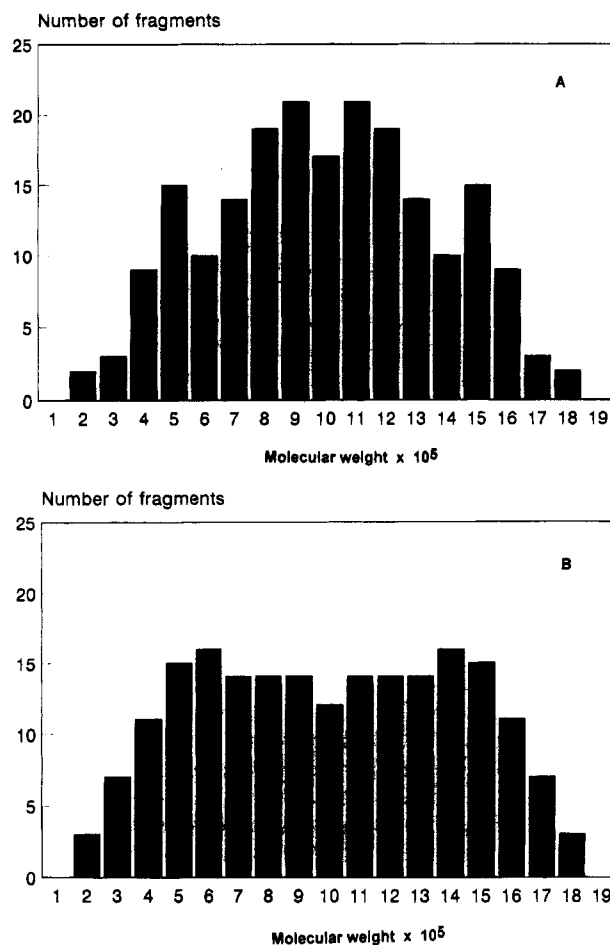


Figure 5. Distribution of molecular weight of the fracture fragments of polystyrene ($M = 2 \times 10^6$). Volumetric flow rate (Q) = 25 cm³/s. (A) Distribution monitored at the orifice. (B) Distribution monitored in the capillary.

to variations in residence times experienced.

In Figure 3 is illustrated how the distribution of molecular weights for the fracture fragments changes, in our simulation experiments, with the residence time of the chain. In Figure 3A the initial distance from the orifice was very small (0.9 mm), corresponding to a short residence time ($5.6 \mu\text{s}$), which is much smaller than the relaxation time of the chain ($73 \mu\text{s}$). We can see that the distribution is quite uniform, indicating that chain scission takes place almost randomly along the chain. This result can be understood taking into consideration that the chain must unfold (with a time constant proportional to the primary relaxation time) in order for the stress to accumulate near the midpoint of the chain. If the chain is not given sufficient time to experience this process, a stress high enough for fracture can accumulate in any segment. In Figure 3B the initial distance from the orifice was high (5 mm), corresponding to a longer residence time ($964 \mu\text{s}$), much longer than the relaxation time of the chain. In this case the distribution is centered more around the midpoint of the chain, since the chain is given more time to fold out and to accumulate the stress in its center before fracture.

After this look at the influence of the initial position, we went to study the fracture yield vs flow rate and the molecular weight distribution of the polymer fragments in the orifice and inside the needle, i.e., in experimentally accessible conditions. The polymer chains were initially placed at a distance of about 2 relaxation times from the orifice, in order to obtain saturation with

respect to fracture yield. The initial molecular weight of the polymer chains used for simulating the Brownian trajectories was the same as mentioned above (2×10^6). The flow rate was $Q = 25 \text{ cm}^3/\text{s}$. The accounting of molecular weight fragments was made at two sites in the device: at the orifice (A) and at a point inside the capillary (B), as explained in the Model and Simulation Method section.

In Figure 4 we present the simulation results for the degradation yield, that is, the percentage of broken chains, vs the flow rate through the syringe, determined at the two points A and B. At the orifice (A), the results are very similar to the experimental results of Nguyen and Kausch, showing that there is no fracture below a critical flow rate (which in the figure is seen to be about $5 \text{ cm}^3/\text{s}$). However, the degradation yield measured at point B is much higher; many chains that survive the passage through the orifice break when they travel downstream in the capillary.

In Figure 5 is shown the simulation results for the size distribution of the fragments (intact chains are not included in the distribution), determined again at the two points A and B. We note that the fragment distribution at the orifice (A) is peaked at about half of the initial molecular weight, indicating that chain scission occurs preferentially at the middle of the chain, as observed in the laboratory experiments mentioned earlier.^{1,2} However, if the simulation proceeds and the size distribution is monitored at some point in the capillary (B), sufficiently far from the orifice, we find a broader, more uniform distribution.

Our interpretation of these results is that the energy that is stored by the polymer molecules in the strong sink flow is later dissipated slowly along the capillary, during a time on the order of the relaxation time. During this time, the energy fluctuates between the various springs and may randomly accumulate in one

of them, not necessarily in the middle one. Thus, more chains are broken when they flow along the capillary, and the distribution of fracture sites is more uniform.

In conclusion, applying the Brownian dynamics simulation technique we have been able in this preliminary study to reproduce the most important aspects of the degradation experiments in transient elongational flow. Furthermore, it is seen that such aspects may be rather dependent on the instrumental parameters, so that what is observed in a specific device may not be valid in other situations.

Acknowledgment. We acknowledge the support from Grants PB93-1132 (DGCYT-MEC) and PIB94-07 (DGEU-CARM). K.D.K. acknowledges Grant ERBCH-BICT 940974 from the Commission of the European Communities. J.J.L.C. acknowledges the award of an FPI-MEC fellowship.

References and Notes

- (1) Reese, H. R.; Zimm, B. H. *J. Chem. Phys.* **1990**, *92*, 2650.
- (2) Nguyen, T. Q.; Kausch, H. H. *Macromolecules* **1990**, *23*, 5137.
- (3) de Gennes, P.-G. *J. Chem. Phys.* **1974**, *60*, 5030.
- (4) Keller, A.; Odell, A. *Colloid Polym. Sci.* **1985**, *263*, 181.
- (5) López Cascales, J. J.; García de la Torre, J. *J. Chem. Phys.* **1991**, *95*, 9384.
- (6) López Cascales, J. J.; García de la Torre, J. *J. Chem. Phys.* **1992**, *97*, 4549.
- (7) Rabin, Y. *J. Chem. Phys.* **1987**, *86*, 5215.
- (8) Bird, R. B.; Curtiss, C. F.; Armstrong, R. C.; Hassager, O. *Dynamics of Polymeric Liquids. Volume 2. Kinetic Theory*; John Wiley & Sons: New York, 1987; p 159.
- (9) Ermak, D. L.; McCammon, J. A. *J. Chem. Phys.* **1978**, *69*, 1352.
- (10) Iniesta, A.; García de la Torre, J. *J. Chem. Phys.* **1990**, *92*, 2015.
- (11) Yamakawa, H. *J. Chem. Phys.* **1970**, *53*, 436.

MA9462363